# Decoding a Neurofeedback-Modulated Performance State in Presence of a Time-Varying Process Noise Variance

Saman Khazaei, Student Member, IEEE, Md Rafiul Amin, Member, IEEE, and Rose T. Faghih, Senior Member, IEEE

Abstract—Everyday life actuators such as music can be used as neurofeedback to improve quality of life and performance. To track one's performance, we develop a performance decoder that captures the time-varying nature of the process noise. We first design a performance state-space model within an autoregressive conditional heteroskedasticity (ARCH) framework to enable adaptive performance state estimation. Then, we design an expectation-maximization algorithm to decode a hidden performance state and estimate the model parameters. Particularly, by considering the sequence of responses and the corresponding reaction times as the observation vector, we employ particle-filtering to track the hidden performance state. We investigate the decoder's performance on experimental data. The estimated performance state is aligned with different task difficulty levels. During the experiment, music was used as neurofeedback to regulate the arousal. Our results indicate music can be utilized to regulate arousal and modulate performance in smart environments. Adaptive performance estimation in varying environments in presence of neurofeedback is a key step for improving performance in real-world settings. Envisioned cyber-physical systems applications include improving productivity in smart workplaces and enhancing learning in online educational systems.

# I. INTRODUCTION

The word cognition refers to the mental action of acquiring knowledge and understanding through thought and experience, which emphasizes the dynamics of learning as opposed to the participant's previous knowledge [1]. Human cognitive functions can be described by two branches, namely basic cognitive functions and higher-level cognitive functions [2]. Basic cognitive functions are composed of attention, working memory (WM), and perception while higher-level cognitive functions comprise speech and language, decision making, and executive control [2]. In this research, cognitive performance during a working memory experiment (*n*-back task) is the topic of interest. Working memory can be described as a function in the brain that retains sensory perceptions for processing and understanding a cognitive task [3]. Studies have displayed that human cognitive performance can be

This work was supported in part by by the U.S. National Science Foundation under grants 1942585/2226123 – CAREER: MINDWATCH: Multimodal Intelligent Noninvasive brain state Decoder for Wearable AdapTive Closed-loop arcHitectures and 1755780 – CRII: CPS: Wearable-Machine Interface Architecture.

S. Khazaei and R. T. Faghih are with the Department of Biomedical Engineering, New York University, New York, NY 10010 USA. S. Khazaei, M.R. Amin, and R. T. Faghih are with the Department of Electrical and Computer Engineering, University of Houston, Houston, TX 77004 USA (e-mail: rfaghih@nyu.edu). Rose T. Faghih served as the senior author.

affected by several external and internal factors such as environmental and psychological components [3]–[5]. Hence, the ability to automatically track the performance and detect the actuators' influences could have extensive applications in designing future cyber-physical systems related to learning and productivity.

The effects of music on human mental states have been receiving increased clinical attention over the past years. Particularly, researchers have been focused on investigating the impacts of music on cognitive performance [6]–[8]. As it has been shown in the arousal-and-mood hypothesis [9]–[11], listening to music may change the cognitive performance of individuals. According to Yerkes–Dodson law, an individual's arousal status is an effective factor that determines the cognitive performance. Hence, music can be applied as a non-invasive actuator to regulate one's arousal state and close the loop with the aim of improving cognitive performance [12], [13].

In order to comprehend the impact of music on performance, there is a demand for modeling the performance state such that it accounts for triggers in a time-varying framework. The performance can be modeled within a statespace approach. State-space methods have been used to model neural processes for a wide range of applications [14]– [32]. In real-world settings, a person's physical surroundings and circumstances may vary significantly throughout the day. Consequently, performance may change with different noise dynamics over time (e.g. work, home, inside a vehicle). Therefore, to track the performance state, we need to design an adaptive estimator that captures the time-varying nature of the process noise. The autoregressive Conditional heteroskedasticity (ARCH) framework [33] has been used successfully in analyzing volatility in financial data. The autoregressive-autoregressive conditional heteroskedasticity (AR-ARCH) model is one of the extensions of the ARCH model which has been used in the state-space scheme [34], [35]. Here, we introduce an AR-ARCH model for the performance states.

One of the informative behavioral data in measuring performance is the sequence of correct and incorrect responses over the experiment which provides information regarding the cognition process. This has been utilized in modeling learning in neuroscience research [4], [5], [24]. The other non-invasive measurement that may constitute the observation set is the response time [36]. Reaction time or response time is the time that the participant takes to observe, evaluate,

and respond to the existing problem. In our case, the time that the participant spends observing a stimulus, identifying that, and pressing a button is forming the reaction time.

For the performance state observations, we present a model that is similar to [36] and consider the correctness of response (binary observation) and reaction time (continuous observation). We model the hidden performance state using an AR-ARCH framework. By considering the AR-ARCH model, we can better capture real-world scenarios. In particular, we can design an adaptive estimator that accounts for the history of the individuals' performance. Thereafter, we monitor the hidden state by applying particle filtering with an expectation-maximization (EM) framework [14], [15], [21], [37]–[40]. Particle filtering is a popular filtering approach that allows handling the nonlinear model's structure and approximating the expected value of the desired function. Based on the observation vector, we generate a set of particles to represent the posterior distribution of some stochastic process at the expectation step (E-step). Next, we implement the maximization step (M-step) with the aim of estimating the unknown model parameters.

### II. METHODS

#### A. Dataset

The dataset was collected from 6 participants between the ages of 22-25. The recorded data comprises functional nearinfrared spectroscopy (fNIRS), electrocardiography (ECG), electrodermal activity (EDA), photoplethysmography (PPG), respiration, and behavioral signals. The participants took part in a working memory experiment called the n-back task [3]. In the n-back task, the participant is presented with a series of stimuli displayed one at a time, and the participant has to identify if the current stimulus is the same as the  $n^{\text{th}}$  previous one [41]. The participant performed equal numbers of 1-back (16 blocks) and 3-back (16 blocks) task blocks during 2 main sessions of calming and exciting background music. The first 5 seconds of each task block were dedicated to task instruction representation. Thereafter, 22 stimuli were implemented in 22 trials with a duration of 2 seconds each. The first 0.5 seconds of each trial were designed for presenting the letter (stimulus) and 1.5 seconds for the participant to respond (total block duration was 49 seconds). At the end of each block, the participant had 10 seconds to relax. Right after the 8th block (halfway mark for each session), the participant relaxed for 20 seconds. Moreover, the participant was given a 2-minute relaxation break between the main two sessions. A detailed description of the experiment is provided in [42].

B. A Performance State-Space Model in Presence of a Time-Varying Process Noise Variance

Assuming the AR-ARCH model for the hidden performance state  $z_i$ , the state-space model can be presented as

$$z_j = z_{j-1} + \epsilon_j, \tag{1}$$

where  $\epsilon_j \sim \mathcal{N}(0, h_j^2)$  is a process noise that follows the ARCH structure. In the ARCH(1) model, we take

$$\epsilon_i = h_i w_i, \tag{2}$$

where

$$h_i^2 = \alpha_0 + \alpha_1 \epsilon_{i-1}^2, \tag{3}$$

refers to the time-varying conditional variance based on the history of the signal. Here,  $\alpha_0$  and  $\alpha_1$  are the model parameters with the constraints on  $\alpha_0>0$  and  $0\leq\alpha_1<1$  [33]. The unconditional and stationary ARCH(1) process variance can be expressed as  $\sigma^2=\frac{\alpha_0}{1-\alpha_1}$ .

Similar to [36], the sequence of responses and the log of reaction time can be considered to form the observation vector. The correct and incorrect response at each trial is shown with  $n_i$ .

Similar to [36], the binary response  $n_j$  can be taken as a Bernoulli-distributed random variable with probability mass function  $p_j^{n_j}(1-p_j)^{1-n_j}$ , where  $p_j=P(n_j=1)$ . We relate  $p_j$  to performance state  $z_j$  using logit transformation [43],

$$\log\left(\frac{p_j}{1 - p_j}\right) = \mu + z_j \Rightarrow p_j = \frac{1}{1 + e^{-(\mu + z_j)}}, \quad (4)$$

where  $\mu$ , is a constant to be determined. Similar to [20], [22], the constant  $\mu$  may be found by considering  $z_j \approx 0$  at the very beginning of the random walk:

$$\mu \approx \log\left(\frac{p_0}{1-p_0}\right),$$
 (5)

where  $p_0$  stands for the average probability of observing correct response during the entire experiment.

The continuous observation equation is

$$r_i = \log t_i = \gamma_0 + \gamma_1 z_i + v_i; \tag{6}$$

where  $t_j$  indicates the reaction time at  $j^{th}$  trial,  $v_j \sim \mathcal{N}(0, \sigma_v^2)$  stands for the noise term, and  $\gamma_0$ ,  $\gamma_1$ , and  $\sigma_v^2$  are the unknown parameters to be estimated.

C. A Performance Decoder Based on the Time-Varying Process Noise Variance

Given the observation vector  $Y^J=\{(n_1,r_1),(n_2,r_2),...,(n_J,r_J)\}$ , the objective is to estimate the performance state  $z_j$  and the unknown model parameters  $\Theta_p=\left[\gamma_0,\gamma_1,\sigma_v^2,\alpha_0,\alpha_1\right]$ , simultaneously. To do so, we employ the expectation-maximization framework. Inspired by [44], we design a particle filter for the AR-ARCH model to decode the hidden performance.

1) E-Step: Following the particle filter design procedure in [44], we design our particle filter to estimate the performance state  $z_j$  in presence of a time-varying ARCH process noise  $\epsilon_j$ . The steps for designing a particle filter are described below

**Step 1:** Initiate the filter by considering K number of particles with the initial variance  $\sigma_0^2$  equal to the stationary value  $\sigma_0^2 = \frac{\alpha_0}{1-\alpha_1}$ , and an arbitrary initial state value.

**Step 2:** Advance the filter from j-1 to j and generate particles  $\hat{z}_j(k)$  based on the derived conditional mean  $\bar{z}_j$ , and conditional variance  $\sigma_j^2$  from the Bayes' rule.

$$\bar{z}_{j}(k) = \frac{\sigma_{j-1}^{2}(k) + h_{j}^{2}(k)}{\gamma_{1}^{2} \left(\sigma_{j-1}^{2}(k) + h_{j}^{2}(k)\right) + \sigma_{v}^{2}} \left[\sigma_{v}^{2} \left(n_{j} - \bar{p}_{j}(k)\right) + \gamma_{1} \left(r_{j} - \gamma_{0} - \gamma_{1}\hat{z}_{j-1}(k)\right)\right] + \hat{z}_{j-1}(k),$$

$$\sigma_{j}^{2}(k) = \left[\frac{1}{\sigma_{j-1}^{2}(k) + h_{j}^{2}(k)} + \bar{p}_{j}(k)\left(1 - \bar{p}_{j}(k)\right) + \frac{\gamma_{1}^{2}}{\sigma_{v}^{2}}\right]^{-1}$$
(8)

where  $h_i^2(k)$  is equivalent to

$$h_j^2(k) = \alpha_0 + \alpha_1 \left(\hat{z}_{j-1}(k) - -\hat{z}_{j-2}(k)\right)^2.$$
 (9)

By plugging  $\bar{p}_j(k) = \left[1 + e^{-(\mu + \bar{z}_j(k))}\right]^{-1}$  in (7),  $\bar{z}_j(k)$  appears on both sides of (7) and we may solve numerically for  $\bar{z}_j(k)$ .

**Step 3:** Assign the importance weight  $w_j(k)$  to the generated  $\hat{z}_j(k)$ . The importance weight density function can take different forms based on the problem of interest; the optimal importance weight  $w_j$  can be derived from

$$w_{j}^{(k)} = \frac{\mathcal{N}\left(Y^{j}; \hat{z}_{j}(k), \sigma_{v}^{2}\right) \mathcal{N}\left(\hat{z}_{j}(k); \hat{z}_{j-1}(k), h_{j}^{2}(k)\right)}{\mathcal{N}\left(\hat{z}_{j}(k); \bar{z}_{j}(k), \sigma_{j}^{2}(k)\right)},$$
(10)

where  $\mathcal{N}(z_{\mathcal{N}}; \mu_{\mathcal{N}}, \sigma_{\mathcal{N}}^2)$  stands for a Gaussian density function of variable  $z_{\mathcal{N}}$  with a mean of  $\mu_{\mathcal{N}}$  and variance of  $\sigma_{\mathcal{N}}^2$  [44].

- **Step 4:** Normalize the weights and perform the resampling. Since we work on a high dimensional problem, particle degeneracy can occur after some iterations and most of the weights concentrate on a few particles. Hence, respmling improves the estimation.
- **Step 5:** Once we reach to j=J, we reverse the direction to obtain a set of smoothed state  $\tilde{z}_j(k)$  with equally smoothed wights  $\tilde{w}_j(k)=1/K$ .
- 2) M-Step: In M-step, model parameters can be estimated such that they maximize the expected value of our log-likelihood function. Similar to [44], [45], we approximate the expected value of the function of interest  $\mathbb{E}[f(z_j)]$  by using the particles and their weights:

$$\mathbb{E}[f(z_j)] \approx \frac{1}{K} \sum_{k=1}^{K} f(\tilde{z}_j(k)). \tag{11}$$

The log-likelihood function (Q) can be written as

$$Q = \sum_{j=1}^{J} \left[ n_{j} (\beta + z_{j}) - \log(1 + e^{\beta + z_{j}}) \right]$$

$$+ \frac{-J}{2} \log(2\pi\sigma_{v}^{2}) - \sum_{j=1}^{J} \frac{(r_{j} - \gamma_{0} - \gamma_{1}z_{j})^{2}}{2\sigma_{v}^{2}}$$

$$+ \frac{-J}{2} \log(2\pi) - \frac{1}{2} \sum_{j=1}^{J} \left[ \frac{(z_{j} - z_{j-1})^{2}}{\alpha_{0} + \alpha_{1}(z_{j-1} - z_{j-2})^{2}} + \log\left(\alpha_{0} + \alpha_{1}(z_{j-1} - z_{j-2})^{2}\right) \right].$$

$$(12)$$

The expected value of Q can be derived from  $(\Pi)$ . Hence, expected value of the log-likelihood function  $(\mathbb{E}[Q])$  can be calculated as follow.

(9) 
$$\mathbb{E}[Q] \approx \sum_{j=1}^{J} \sum_{k=1}^{K} \frac{1}{K} \left[ n_{j} \left( \beta + \tilde{z}_{j}(k) \right) - \log \left( 1 + e^{\beta + \tilde{z}_{j}(k)} \right) \right]$$
(13)
$$- \frac{1}{K} \left[ \frac{J}{2} \log(2\pi\sigma_{v}^{2}) + \sum_{j=1}^{J} \sum_{k=1}^{K} \frac{\left( r_{j} - \gamma_{0} - \gamma_{1} \tilde{z}_{j}(k) \right)^{2}}{2\sigma_{v}^{2}} \right]$$
the can the
$$- \frac{1}{K} \left[ \frac{J}{2} \log(2\pi) + \sum_{j=1}^{J} \sum_{k=1}^{K} \left[ \frac{\left( \tilde{z}_{j}(k) - \tilde{z}_{j-1}(k) \right)^{2}}{\alpha_{0} + \alpha_{1} \left( \tilde{z}_{j-1}(k) - \tilde{z}_{j-2}(k) \right)^{2}} \right]$$

$$+ \log \left( \alpha_{0} + \alpha_{1} \left( \tilde{z}_{j-1}(k) - \tilde{z}_{j-2}(k) \right)^{2} \right) \right] .$$

We aim to estimate the unknown parameters  $\hat{\Theta} = [\gamma_0, \gamma_1, \sigma_v^2, \hat{\alpha}_0, \hat{\alpha}_1]$  such that they maximize  $\mathbb{E}[Q]$ . Hence,  $\gamma_0, \gamma_1$ , and  $\sigma_v^2$  can be recovered from:

$$\frac{\partial \mathbb{E}[Q]}{\partial \gamma_0} = 0$$

$$0 = K \sum_{j=1}^{J} r_j - KJ\gamma_0 - \gamma_1 \sum_{j=1}^{J} \sum_{k=1}^{K} \tilde{z}_j(k)$$

$$\gamma_0 = \frac{K \sum_{j=1}^{J} r_j - \gamma_1 \sum_{k=1}^{K} \sum_{j=1}^{J} \tilde{z}_j(k)}{KJ},$$
(14)

where  $\gamma_1$  may be obtained from

$$\frac{\partial \mathbb{E}[Q]}{\partial \gamma_1} = 0$$

$$0 = \sum_{j=1}^{J} \sum_{k=1}^{K} \left( r_j \tilde{z}_j(k) - \gamma_0 \tilde{z}_j(k) - \gamma_1 \tilde{z}_j^2(k) \right)$$

$$\gamma_1 = \left[ \frac{\sum_{j=1}^{J} \sum_{k=1}^{K} \left( \tilde{z}_j(k) \sum_{j=1}^{J} \sum_{k=1}^{K} \tilde{z}_j(k) \right)}{KJ} \right]$$
(15)

$$-\sum_{j=1}^{J} \sum_{k=1}^{K} \left( \tilde{z}_{j}^{2}(k) \right) \right]^{-1} \left[ \frac{1}{J} \sum_{J=1}^{J} \sum_{k=1}^{K} \left( \tilde{z}_{j}(k) \sum_{j=1}^{J} r_{j} \right) - \sum_{j=1}^{J} \sum_{k=1}^{K} \left( r_{j} \tilde{z}_{j}(k) \right) \right],$$

and  $\sigma_v^2$  can be written as

$$\frac{\partial \mathbb{E}[Q]}{\partial \sigma_v^2} = 0$$

$$\sigma_v^2 = \frac{1}{KJ} \sum_{k=1}^K \sum_{i=1}^J \left[ \left( r_j - \gamma_0 - \gamma_1 \tilde{z}_j(k) \right)^2 \right].$$
(16)

Also, we find the ARCH unknown parameters with MAT-LAB function fmincon such that they optimize the cost function L

$$L = \sum_{j=1}^{J} \sum_{k=1}^{K} \left[ \frac{\left(\tilde{z}_{j}(k) - \tilde{z}_{j-1}(k)\right)^{2}}{\alpha_{0} + \alpha_{1}\left(\tilde{z}_{j-1}(k) - \tilde{z}_{j-2}(k)\right)^{2}} + \log\left(\alpha_{0} + \alpha_{1}\left(\tilde{z}_{j-1}(k) - \tilde{z}_{j-2}(k)\right)^{2}\right) \right].$$
(17)

Figure I shows the scheme of the proposed performance state decoder. We iterate between the E-step and the M-step until meeting convergence criteria.

## III. RESULTS AND DISCUSSION

In this section, we assess the impact of music as a type of neurofeedback to modulate performance. In particular, we utilize the AR-ARCH performance state decoder to analyze experimental data.

The simplest approach to evaluate the music's impact on cognitive performance is to compare the sequence of correct/incorrect responses during different sections of the experiment. Figure 2 represents the sequence of incorrect responses during calming and exciting sessions for six participants, separately; a sub-panel with more blue vertical lines is equivalent to a higher number of incorrect responses throughout a session.

Since we account for the reaction time in shaping the observation vector, it is important to analyze the variations in individuals' reaction time based on the background music. In Fig. 3, we display the distribution of participants' reaction times during calming and exciting sessions by using box plots.

The performance state decoder's results for one participant are illustrated in Fig. 4. The first subplot shows the log of reaction time with the black dots and the blue curve shows the reconstructed observation ( $\tilde{r}_j = \gamma_0 + \gamma_1 \tilde{z}_j$ ) from the estimated state  $\tilde{z}_j$  ( $R^2 = 0.92$ ). The second subplot displays the estimated performance state and the number of correct responses at each block. The mean performance state value for the calming session is 0.54 while the mean performance at the exciting session is 0.79. The third and fourth subplots depend directly on the estimated performance

state value such that the third subplot demonstrates the probability of having a correct response  $p_j$ , and the fourth subplot shows the high performance index (HPI) derived as  $p(z_j > z_{\rm threshold})$ . We set the threshold to the median of estimated states.

We focus on the estimated performance state's distribution through calming and exciting sessions. Figure 5 presents the box plots for the performance states during calming and exciting sessions, respectively. The comparison of the data based on background music is done by considering the difference between the median of the distributions.

According to the obtained results in Fig. 2, we can observe that for all the participants except participant number two, the red regions of subplots that refer to exciting sessions have fewer incorrect responses (blue vertical lines) compared to the green regions (calming). Potentially, for these participants, the exciting music session (high arousal session) helps them reach a psychological state in which they feel entirely absorbed in the task. The fact that participant two does not follow a similar trend reveals that the result might change based on the individual's baselines. Perhaps, participant two is more sensitive and becomes aroused more easily in comparison to other participants. Given the reaction time distribution in Fig. 3 and the connection between the median of calming and exciting sessions' data, we can detect that the exciting music provokes all six participants to react faster. This finding conforms with the results in [46] where it has been shown that caffeine, which is associated with higher arousal, improved the reaction time.

In the first subplot of Fig. 4, we can observe the agreement between the experimental reaction time data (continuous observation  $r_i$ ) and the reconstructed reaction time. In the second subplot, there are high fluctuations in the estimated states, which can be a result of implementing the ARCH process noise in modeling the performance state. Furthermore, states in blocks with darker background colors (3-back tasks) have lower levels since performing the 3-back task is more difficult compared to the 1-back task. Introducing the ARCH process noise enables the filter to capture the environmental changes and produce volatile state estimation. The volatility in the last five blocks of the experiment is consecutively high, which can be modeled by including the ARCH process noise. An experiment with more sessions and longer duration would enable a more comprehensive investigation of the ARCH process noise. Overall, for participant 1 (Fig. 4), we can observe that the baseline of the estimated state, probability of having a correct response, and HPI are higher during the exciting music session (higher arousal) compared to the calming music session (lower arousal). For this particular participant, high arousal music possibly improves working memory performance. These findings are consistent with the observed number of correct responses and reaction time for this participant. As explained in [47], since the model has a high degree of freedom with a small number of samples, it is possible to overfit and align closely to the continuous observation (reaction time). Hence, in some blocks, we can detect that the algorithm tends to specify more weight to

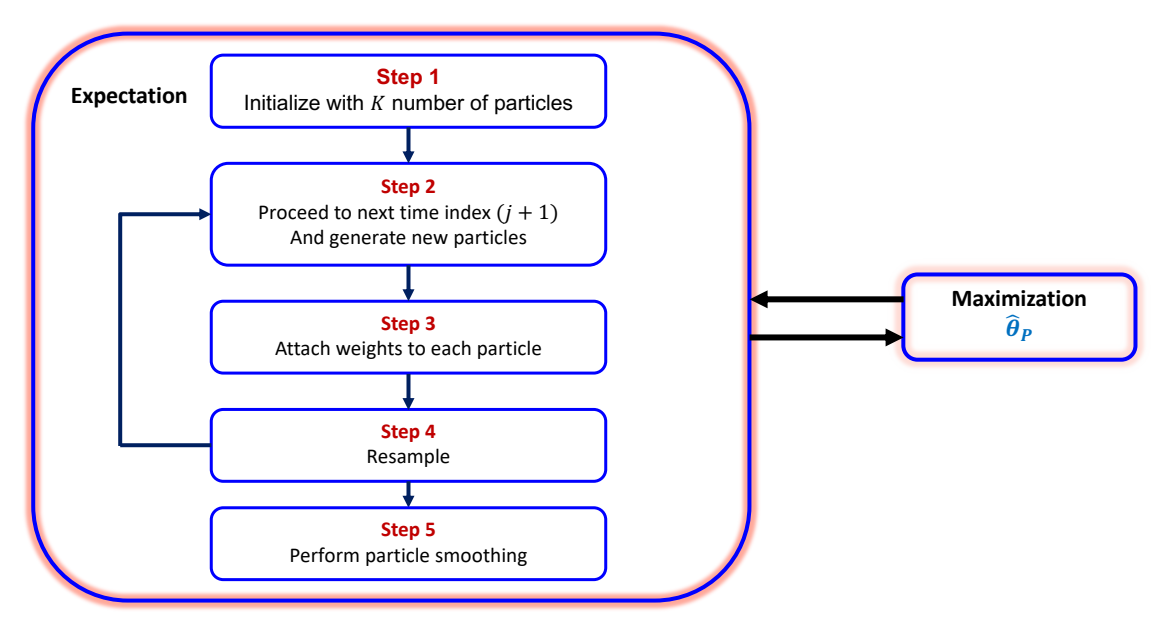


Fig. 1: An overview of the designed performance decoder. The proposed decoder consists of two major steps, namely, the expectation and the maximization steps. The algorithm iterates between the E-step and the M-step until convergence.

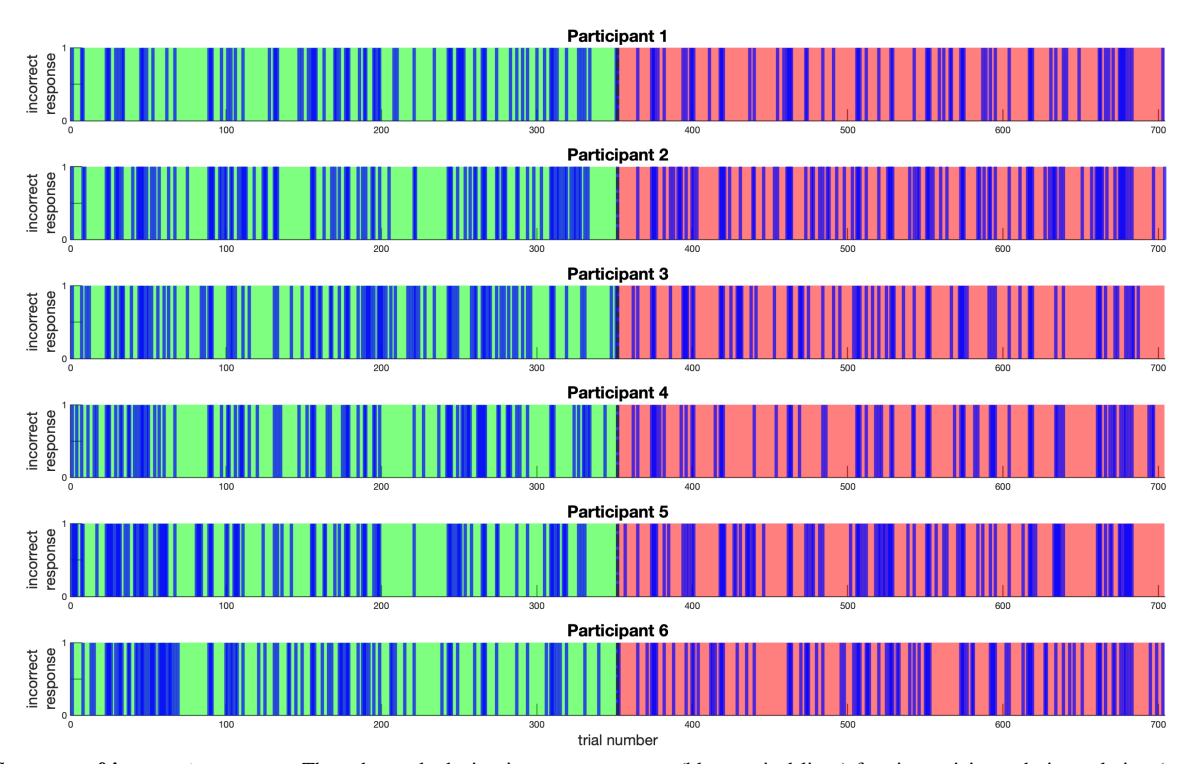


Fig. 2: Sequence of incorrect responses. The sub-panels depict: incorrect responses (blue vertical lines) for six participant during calming (green) and exciting (red) sessions respectively; The x-axis specifies the trail number.

reaction time rather than the sequence of responses. One possible approach to improve the condition is to use early stopping while it increases the risk of deviation.

According to the estimated performance box plots in Fig. 5. overall, the cognitive performance improves for all six participants during the exciting session. However, the amount of improvement varies for each participant, which may reveal differences in their cognition process and a demand for a

person-specific performance decoder.

# IV. CONCLUSION AND FUTURE DIRECTION

The main objective of this research is to evaluate music as a potential neurofeedback mechanism for designing closedloop architectures and improving performance. According to our results, music can impact the participant's cognitive performance [6]. One should note that the type of music, and the

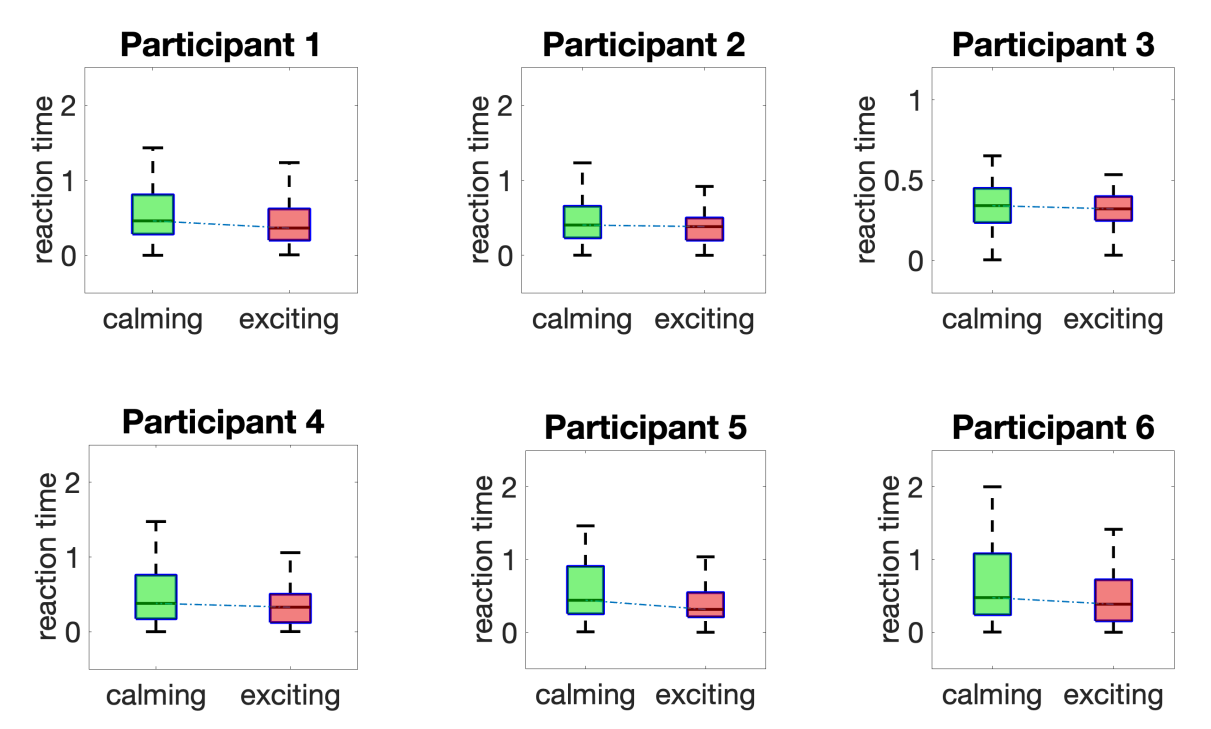


Fig. 3: Reaction time distribution. The sub-panels represent the reaction time box plots for six participant during calming (green) and exciting (red) sessions, respectively. The blue dashed line connects the median of the calming session data to the median of the exciting session data.

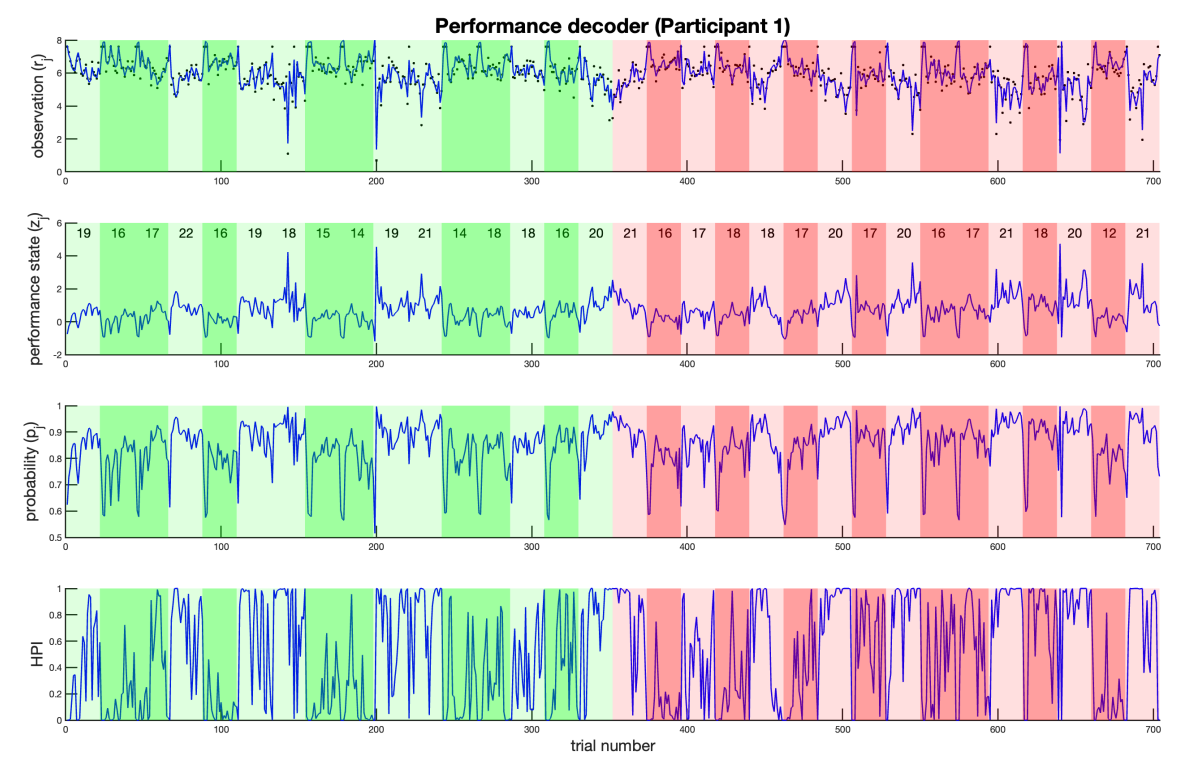


Fig. 4: Performance state estimation for one participant. The subplots respectively show: the reaction time (black dots) and reconstructed reaction time (blue curve); the state estimate (blue curve) and number of correct responses at each block (numbers at the top of the second sub-panel); estimated Probabilities of observing correct response  $p_j$ ; the high performance index or HPI. The background colors in each sub-panel mark: the 1-back task during the calming session (light green); the 3-back task during the exciting session (light red); the 3-back task during the exciting session (dark red).

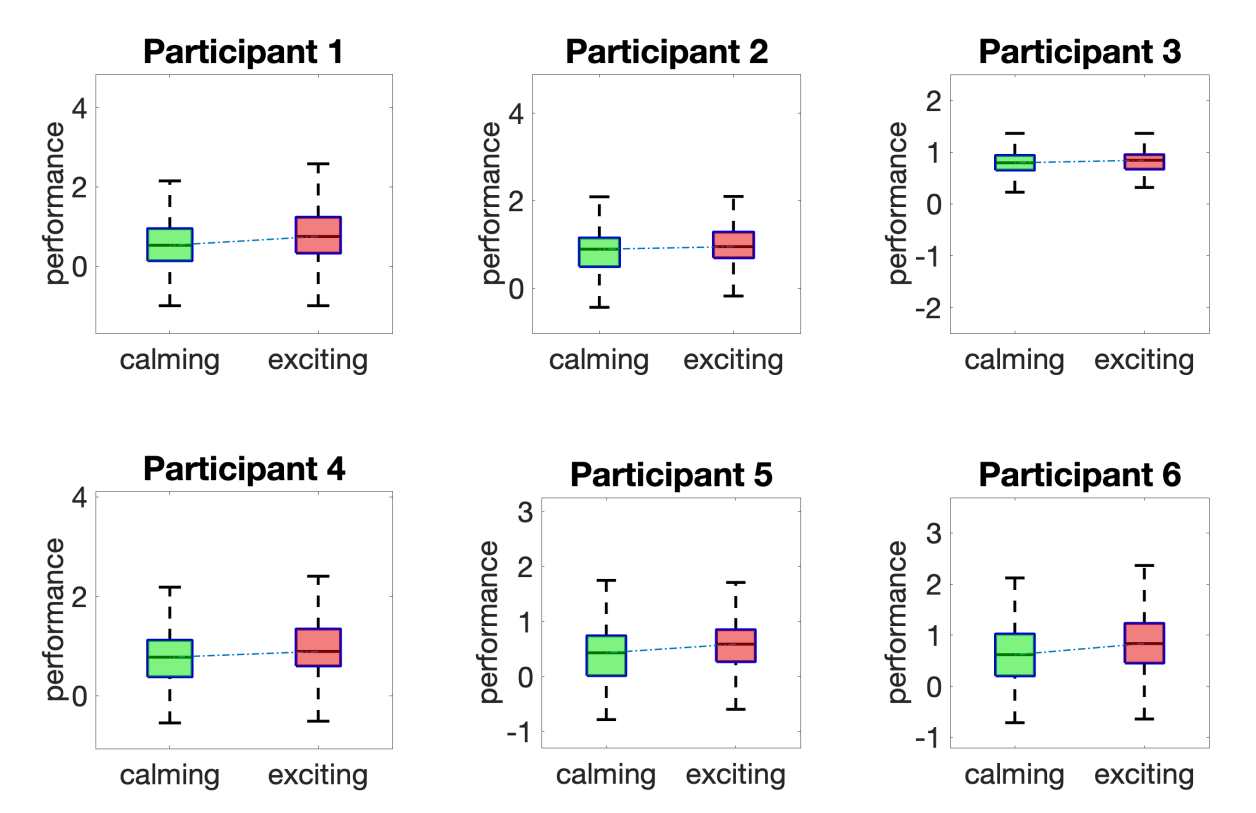


Fig. 5: Performance state distribution. The sub-panels represent the performance state box plots for six participants during calming (green) and exciting (red) sessions, respectively. The blue dashed line connects the median of the calming session data to the median of the exciting session data.

individual's familiarity and emotional baseline can influence how music can be used as neurofeedback in a person-specific manner. In [3], we have quantitatively illustrated that one's cognitive performance is a function of arousal level, and hence, regulation of arousal can modulate performance. Our results indicate that music can be used as a non-invasive actuator in a closed-loop manner. However, the number of participants is limited for making any general conclusions and the future directions of this research include collecting a larger dataset.

In the future, we plan to implement a longer experiment with a higher number of participants that offers us more information regarding the history of the signals and their impacts on the current states. More specifically, the ARCH model might be applied to data that is stored for a longer period. Furthermore, we are interested in designing cognitive experiments that consider multiple psychological factors such as variation in both light and music. In order to implement a controller, several approaches can be employed [48]–[50]. Since individuals' responses to actuators may vary, and the performance baseline of each person is different, we plan to personalize the state-space model by adding uncertainty to the model parameters.

### **ACKNOWLEDGMENT**

The authors thank Dilranjan S. Wickramasurya and Srinidhi Parshi for their help during data collection and preparation of the dataset.

### REFERENCES

- N. J. Cooke, "Varieties of knowledge elicitation techniques," *International journal of human-computer studies*, vol. 41, no. 6, pp. 801–849, 1994.
- [2] E. L. Glisky, "Changes in cognitive function in human aging," *Brain aging*, pp. 3–20, 2007.
- [3] S. Khazaei, M. R. Amin, and R. T. Faghih, "Decoding a neurofeedback-modulated cognitive arousal state to investigate performance regulation by the yerkes-dodson law," in 2021 43rd Annual International Conference of the IEEE Engineering in Medicine & Biology Society (EMBC), pp. 6551–6557, IEEE, 2021.
- [4] C. Kirschbaum, O. T. Wolf, M. May, W. Wippich, and D. H. Hell-hammer, "Stress-and treatment-induced elevations of cortisol levels associated with impaired declarative memory in healthy adults," *Life sciences*, vol. 58, no. 17, pp. 1475–1483, 1996.
- [5] B. K. Hawes, T. T. Brunyé, C. R. Mahoney, J. M. Sullivan, and C. D. Aall, "Effects of four workplace lighting technologies on perception, cognition and affective state," *International Journal of Industrial Ergonomics*, vol. 42, no. 1, pp. 122–128, 2012.
- [6] M. R. Amin, M. Tahir, and R. T. Faghih, "A state-space investigation of impact of music on cognitive performance during a working memory experiment," in 2021 43rd Annual International Conference of the IEEE Engineering in Medicine & Biology Society (EMBC), pp. 757– 762, IEEE, 2021.
- [7] Y. Jing, S. Jing, C. Huajian, S. Chuangang, and L. Yan, "The gender difference in distraction of background music and noise on the cognitive task performance," in 2012 8th International Conference on Natural Computation, pp. 584–587, IEEE, 2012.
- [8] M. Nithya.S, "Analysis of music effect on n-back task performance," pp. 38–42, 2016.
- [9] W. F. Thompson, E. G. Schellenberg, and G. Husain, "Arousal, mood, and the mozart effect," *Psychological science*, vol. 12, no. 3, pp. 248– 251, 2001.
- [10] G. Husain, W. F. Thompson, and E. G. Schellenberg, "Effects of musical tempo and mode on arousal, mood, and spatial abilities," *Music perception*, vol. 20, no. 2, pp. 151–171, 2002.

- [11] E. G. Schellenberg, T. Nakata, P. G. Hunter, and S. Tamoto, "Exposure to music and cognitive performance," *Psychology of Music*, vol. 35, no. 1, pp. 5–19, 2007.
- [12] R. M. Yerkes, J. D. Dodson, et al., "The relation of strength of stimulus to rapidity of habit-formation," 1908.
- [13] R. M. Yerkes, The dancing mouse, vol. 1. Macmillan Company, 1907.
- [14] D. S. Wickramasuriya, L. J. Crofford, A. S. Widge, and R. T. Faghih, "Hybrid decoders for marked point process observations and external influences," *IEEE Transactions on Biomedical Engineering*, 2022.
- [15] D. S. Wickramasuriya and R. T. Faghih, "A mixed filter algorithm for sympathetic arousal tracking from skin conductance and heart rate measurements in pavlovian fear conditioning," *PloS one*, vol. 15, no. 4, p. e0231659, 2020.
- [16] D. S. Wickramasuriya and R. T. Faghih, "A marked point process filtering approach for tracking sympathetic arousal from skin conductance," *IEEE Access*, vol. 8, pp. 68499–68513, 2020.
- [17] D. D. Pednekar, M. R. Amin, H. F. Azgomi, K. Aschbacher, L. J. Crofford, and R. T. Faghih, "Characterization of cortisol dysregulation in fibromyalgia and chronic fatigue syndromes: a state-space approach," *IEEE Transactions on Biomedical Engineering*, vol. 67, no. 11, pp. 3163–3172, 2020.
- [18] T. Yadav, M. M. U. Atique, H. F. Azgomi, J. T. Francis, and R. T. Faghih, "Emotional valence tracking and classification via state-space analysis of facial electromyography," in 2019 53rd Asilomar Conference on Signals, Systems, and Computers, pp. 2116–2120, IEEE, 2019.
- [19] M. B. Ahmadi, A. Craik, H. F. Azgomi, J. T. Francis, J. L. Contreras-Vidal, and R. T. Faghih, "Real-time seizure state tracking using two channels: A mixed-filter approach," in 2019 53rd Asilomar Conference on Signals, Systems, and Computers, pp. 2033–2039, IEEE, 2019.
- [20] D. S. Wickramasuriya and R. T. Faghih, "A bayesian filtering approach for tracking arousal from binary and continuous skin conductance features," *IEEE Transactions on Biomedical Engineering*, vol. 67, no. 6, pp. 1749–1760, 2019.
- [21] D. S. Wickramasuriya and R. T. Faghih, "A novel filter for tracking real-world cognitive stress using multi-time-scale point process observations," in 2019 41st Annual International Conference of the IEEE Engineering in Medicine and Biology Society (EMBC), pp. 599–602, IEEE, 2019.
- [22] D. S. Wickramasuriya, M. Amin, and R. T. Faghih, "Skin conductance as a viable alternative for closing the deep brain stimulation loop in neuropsychiatric disorders," *Frontiers in neuroscience*, vol. 13, p. 780, 2019
- [23] D. S. Wickramasuriya, C. Qi, and R. T. Faghih, "A state-space approach for detecting stress from electrodermal activity," in 2018 40th Annual International Conference of the IEEE Engineering in Medicine and Biology Society (EMBC), pp. 3562–3567, IEEE, 2018.
- [24] A. C. Smith, L. M. Frank, S. Wirth, M. Yanike, D. Hu, Y. Kubota, A. M. Graybiel, W. A. Suzuki, and E. N. Brown, "Dynamic analysis of learning in behavioral experiments," *Journal of Neuroscience*, vol. 24, no. 2, pp. 447–461, 2004.
- [25] A. C. Smith, M. R. Stefani, B. Moghaddam, and E. N. Brown, "Analysis and design of behavioral experiments to characterize population learning," *Journal of Neurophysiology*, vol. 93, no. 3, pp. 1776–1792, 2005.
- [26] T. P. Coleman, M. Yanike, W. A. Suzuki, and E. N. Brown, "A mixed-filter algorithm for dynamically tracking learning from multiple behavioral and neurophysiological measures," *The dynamic brain: An* exploration of neuronal variability and its functional significance, pp. 3–28, 2011.
- [27] X. Deng, R. T. Faghih, R. Barbieri, A. C. Paulk, W. F. Asaad, E. N. Brown, D. D. Dougherty, A. S. Widge, E. N. Eskandar, and U. T. Eden, "Estimating a dynamic state to relate neural spiking activity to behavioral signals during cognitive tasks," in 2015 37th Annual International Conference of the IEEE Engineering in Medicine and Biology Society (EMBC), pp. 7808–7813, IEEE, 2015.
- [28] M. M. Shanechi, R. C. Hu, M. Powers, G. W. Wornell, E. N. Brown, and Z. M. Williams, "Neural population partitioning and a concurrent brain-machine interface for sequential motor function," *Nature neuroscience*, vol. 15, no. 12, pp. 1715–1722, 2012.
- [29] H. F. Azgomi and R. T. Faghih, "A wearable brain machine interface architecture for regulation of energy in hypercortisolism," in 2019 53rd Asilomar Conference on Signals, Systems, and Computers, pp. 254– 258, IEEE, 2019.
- [30] M. M. Shanechi, R. C. Hu, and Z. M. Williams, "A cortical-spinal

- prosthesis for targeted limb movement in paralysed primate avatars," *Nature communications*, vol. 5, no. 1, pp. 1–9, 2014.
- [31] L. R. Branco, A. Ehteshami, H. F. Azgomi, and R. T. Faghih, "Closed-loop tracking and regulation of emotional valence state from facial electromyogram measurements," *Frontiers in computational neuroscience*, vol. 16, p. 747735, 2022.
- [32] S. Lee, H. B. Hwang, S. Park, S. Kim, J. H. Ha, Y. Jang, S. Hwang, H.-K. Park, J. Lee, and I. Y. Kim, "Mental stress assessment using ultra short term hrv analysis based on non-linear method," *Biosensors*, vol. 12, no. 7, p. 465, 2022.
- [33] R. F. Engle, "Autoregressive conditional heteroscedasticity with estimates of the variance of united kingdom inflation," *Econometrica: Journal of the econometric society*, pp. 987–1007, 1982.
- [34] D. B. Cline and H. P. Huay-min, "Stability and the lyapounov exponent of threshold ar-arch models," *The Annals of Applied Probability*, vol. 14, no. 4, pp. 1920–1949, 2004.
- [35] R. Giacometti, M. Bertocchi, S. T. Rachev, and F. J. Fabozzi, "A comparison of the lee-carter model and ar-arch model for forecasting mortality rates," *Insurance: Mathematics and Economics*, vol. 50, no. 1, pp. 85–93, 2012.
- [36] M. J. Prerau, A. C. Smith, U. T. Eden, Y. Kubota, M. Yanike, W. Suzuki, A. M. Graybiel, and E. N. Brown, "Characterizing learning by simultaneous analysis of continuous and binary measures of performance," *Journal of neurophysiology*, vol. 102, no. 5, pp. 3060–3072, 2009.
- [37] D. S. Wickramasuriya, C. A. Perumalla, K. Davaslioglu, and R. D. Gitlin, "Base station prediction and proactive mobility management in virtual cells using recurrent neural networks," in 2017 IEEE 18th Wireless and Microwave Technology Conference (WAMICON), pp. 1–6, IEEE, 2017.
- [38] A. Yaghmour, M. R. Amin, and R. T. Faghih, "Decoding a music-modulated cognitive arousal state using electrodermal activity and functional near-infrared spectroscopy measurements," in 2021 43rd Annual International Conference of the IEEE Engineering in Medicine & Biology Society (EMBC), pp. 1055–1060, IEEE, 2021.
- [39] D. S. Wickramasuriya and R. T. Faghih, "A cortisol-based energy decoder for investigation of fatigue in hypercortisolism," in 2019 41st Annual International Conference of the IEEE Engineering in Medicine and Biology Society (EMBC), pp. 11–14, IEEE, 2019.
- [40] R. Amin and R. T. Faghih, "Physiological characterization of electrodermal activity enables scalable near real-time autonomic nervous system activation inference," *PLoS computational biology*, vol. 18, no. 7, p. e1010275, 2022.
- [41] S. Parshi, R. Amin, H. F. Azgomi, and R. T. Faghih, "Mental workload classification via hierarchical latent dictionary learning: A functional near infrared spectroscopy study," in 2019 IEEE EMBS International Conference on Biomedical & Health Informatics (BHI), pp. 1–4, IEEE, 2019
- [42] S. Parshi, "A functional-near infrared spectroscopy investigation of mental workload," Master's thesis, University of Houston, 2020.
- [43] P. McCullagh and J. Nelder, "Generalized linear models, baton rouge, la," 1989.
- [44] J.-C. Duan and A. Fulop, "A stable estimator of the information matrix under em for dependent data," *Statistics and Computing*, vol. 21, no. 1, pp. 83–91, 2011.
- [45] J. F. de Freitas, M. Niranjan, A. H. Gee, and A. Doucet, "Sequential monte carlo methods to train neural network models," *Neural computation*, vol. 12, no. 4, pp. 955–993, 2000.
- [46] H. R. Lieberman, W. J. Tharion, B. Shukitt-Hale, K. L. Speckman, and R. Tulley, "Effects of caffeine, sleep loss, and stress on cognitive performance and mood during us navy seal training," *Psychopharma-cology*, vol. 164, no. 3, pp. 250–261, 2002.
- [47] C. M. Bishop and N. M. Nasrabadi, Pattern recognition and machine learning, vol. 4. Springer, 2006.
- [48] H. F. Azgomi, D. S. Wickramasuriya, and R. T. Faghih, "State-space modeling and fuzzy feedback control of cognitive stress," in 2019 41st Annual International Conference of the IEEE Engineering in Medicine and Biology Society (EMBC), pp. 6327–6330, IEEE, 2019.
- [49] H. F. Azgomi, I. Cajigas, and R. T. Faghih, "Closed-loop cognitive stress regulation using fuzzy control in wearable-machine interface architectures," *IEEE Access*, vol. 9, pp. 106202–106219, 2021.
- [50] H. F. Azgomi and R. T. Faghih, "Enhancement of closed-loop cognitive stress regulation using supervised control architectures," *IEEE Open Journal of Engineering in Medicine and Biology*, vol. 3, pp. 7– 17, 2022.